JOURNAL OF MATERIALS SCIENCE **35** (2000) 3269–3278

Influence of the synthesis methods on the physical and structural characteristics of $0.6TiO_2 \cdot 0.4Al_2O_3$ catalytic supports

R. LINACERO, M. L. ROJAS-CERVANTES*, J. DE D. LÓPEZ-GONZÁLEZ
Departamento de Química Inorgánica y Química Técnica, Facultad de Ciencias (U.N.E.D.); Paseo Senda del Rey nº 9, Madrid 28.040-Spain
E-mail: mrojas@ccia.uned.es

A series of $0.6TiO_2 \cdot 0.4Al_2O_3$ catalytic supports has been prepared by both non-hydrolytic route and hydrolytic sol-gel processes. Some synthesis variables, such as the use of ethylene glycol as complexing agent, the generation in situ of the hydrolysis water, or the separated hydrolysis of the respective alkoxides, have been studied for the samples prepared by the hydrolytic sol-gel method. The physical and structural characterisation of the samples has been carried out by different techniques. The textural results show that the surface area and the pore size distribution are influenced by the synthesis method, which also affects the thermal behaviour and the crystallization process of the samples. The distribution of acid sites is also different, depending on the synthesis conditions.

1. Introduction

The sol-gel process, which comprises the controlled hydrolysis and subsequent condensation of metal alkoxides, offers new approaches to the synthesis of highly porous oxide materials. Each step of the process can be controlled and modified in order to obtain a specific material, with better characteristics from the catalytic point of view than those obtained by the traditional methods of preparation [1]. One of the most interesting applications of the sol-gel process can be found in the field of catalysis, not only for the preparation of supports [2–4], but also for the synthesis of supported metal oxide catalysts, starting from an homogeneous solution containing both the metal precursor and the support precursor [5–8].

There are numerous variables which affect the reaction rates and the uniformity of the hydrolysis and polimerization [9], influencing on the physical and structural characteristics of the obtained oxides [10]. Recently, Andrianainarivelo *et al.* [11] have reported a new sol-gel route, involving no hydrolysis, for the preparation of binary oxides, which is very efficient to achieve gels with a high degree of homogeneity. In the present paper, we have applied a similar non-hydrolytic method for the synthesis of the $0.6TiO_2 \cdot 0.4Al_2O_3$ mixed oxide. This paper could be considered as a continuation of the one reporting the synthesis via sol-gel of the $xTiO_2 \cdot (1-x)Al_2O_3$ series, with different molar ratios ($x = 0.0$, 0.2, 0.5, 0.6, 0.8 and 1.0) [12]. The support with $x = 0.6$ molar ratio has been chosen for the present work, because as it will be observed in the reactions describing the non-hydrolytic sol-gel processes, the mixed oxide to be obtained in the stoichiometric conditions employed should have the theoretical composition of $Ti_3Al_4O_{12}$, which is the equivalent to $0.6TiO_2 \cdot 0.4Al_2O_3$, that is, $x = 0.6$. Additionally, the $x = 0.6$ sample is the one containing the combination of Al-Ti acid sites with highest acid strength of all the samples of the $xTiO_2 \cdot (1-x)Al_2O_3$ series studied by us [12]. In order to compare different synthesis methods and to know the influence of these on the physical and structural characteristics of the support obtained, the oxide $x = 0.6$ has also been synthesised by the hydrolytic sol-gel process, but involving the modification of some variables. These variables are: the use of a complexing agent, the generation *in situ* of the hydrolysis water, and the separated hydrolysis of each one of the two alkoxides.

2. Synthesis procedure

2.1. Non-hydrolytic sol-gel route

In conventional sol-gel processes, the formation of sols or gels results from the formation of M-O-M bridges through hydrolysis and polimerization reactions. In the non-hydrolytic sol-gel process, M-O-M or M-O-M′ bridges are obtained by condensation between halide and alkoxide groups, with elimination of alkyl halide. To avoid the use of alkoxides (which are often quite expensive), the alkoxide groups can be formed *in situ* by the etherolysis of the metal halide by an organic ether. In both cases, the stoichiometry of these reactions requires an equal number of alkyl groups and halide groups.

* Author to whom all correspondence should be addressed.

2.1.1. Halide-ether route (phaha)

The preparation of this precursor involves the etherolysis of the metal halide by organic ether, according to the reaction:

$$xMCl_4 + yM'Cl_3 + z(ROR) \rightarrow M_xM'_yO_z \quad \text{with } 4x + 3y = 2z$$

Although the reaction allows different Al/Ti stoichiometries, the theoretical amounts employed in the synthesis of phaha were the following ones:

$$3TiCl_4 + 4AlCl_3 + 12(CH_3)_2\text{-CH-O-CH-}(CH_3)_2 \rightarrow Ti_3Al_4O_{12} + 24(CH_3)_2CHCl$$

which are the appropriate to obtain the mixed oxide $Ti_3Al_4O_{12}$, which is equivalent to the $0.6TiO_2 \cdot (1-x)Al_2O_3$, that is, $x = 0.6$. The diisopropyl ether was chosen because it appeared to be the most effective in term of the degree of condensation of the gel for Zr-Ti oxides [11]. The $AlCl_3$ (solid) was slowly added to the appropriate amount of diisopropyl ether and kept under reflux at 80 C for 30 minutes, until a complete solution. Once the solution was cooled, the $TiCl_4$ was slowly added and the solution was again refluxed and stirred at 70 C, gelling after 30 minutes. The stirring was stopped and the gel was aged for three days, afterwards it was completely dried. Then, the gel was calcined under an air flow of 75 ml·min^{-1}, according to the following calcination program:

$$T_0 = 30\,\text{C}$$
$$r_1 = 3\,\text{C}\cdot\text{min}^{-1} \quad T_1 = 100\,\text{C} \quad t_1 = 30\,\text{min}$$
$$r_2 = 3\,\text{C}\cdot\text{min}^{-1} \quad T_2 = 200\,\text{C} \quad t_2 = 60\,\text{min}$$
$$r_3 = 3\,\text{C}\cdot\text{min}^{-1} \quad T_3 = 500\,\text{C} \quad t_3 = 180\,\text{min}$$

2.1.2. Halide-alkoxide route

This route involves the thermal condensation between a metal halide and a metal alkoxide. It must be taken into account that the condensation competes with the redistribution of the ligands, which usually takes place rapidly at room temperature and leads to a complicated mixture of halogenoalkoxides [13]:

$$MX_n + M(OR)_n \rightarrow MX_x(OR)_{n-x} \quad \text{with } 0 \le x \le n$$

Three precursors have been synthesised by the halide-alkoxide route, two of them employing the titanium tetrachloride and two different aluminium alkoxides, and a third one using titanium isopropoxide and aluminium trichloride. The precursors synthesised were the following ones:

phaTiSecAl

$$3TiCl_4 + 4Al((CH_3)_3\text{C-O})_3 \rightarrow Ti_3Al_4O_{12} + 12(CH_3)_3CCl$$

The aluminium secbutoxide was slowly added to the titanium tetrachloride and the solution was heated and stirred at 100 C, occurring the gellification after 24 h. The gel was aged for 5 days, dried in an oven at 80 C for 14 h, and calcined according to the program explained above.

phaTiIsAl

$$3TiCl_4 + 4Al((CH_3)_2\text{CH-O})_3 \rightarrow Ti_3Al_4O_{12} + 12(CH_3)_2CHCl$$

As the aluminium isopropoxide is a solid, it was previously solved in 25 mL of CCl_4 under reflux at 90 C for 1 h and 20 minutes, until a complete and homogeneous solution. After that, the corresponding amount of titanium tetrachloride was added and the solution was refluxed at 100 C for 24 h. After this time, a gel was not obtained, and the yellowish precipitate formed was filtered, dried and calcined.

pIsTihaAl

$$3Ti((CH_3)_2\text{CH-O})_4 + 4AlCl_3 \rightarrow Ti_3Al_4O_{12} + 12(CH_3)_2CHCl$$

As the aluminium trichloride is a solid, it was also previously solved in 25 mL of CCl_4 under reflux at 90 C for around 4 h, until a homogeneous solution was obtained. Then, the titanium isopropoxide was slowly added and the solution was heated and refluxed at 100 C for 24 h. As in the former case, a grisaceous precipitate was obtained, which was filtered, dried and calcined.

2.2. px06

The synthesis of this gel was described previously [12]. The molar ratios used were alcohol/alkoxide = 15 and water/alkoxide = 5, which are the same used for the rest of the precursors synthesised in other different conditions.

2.3. px06EG

A route involving the (co)polimerization of the alkoxides with ethylene glycol was used for the synthesis of this precursor. The ethylene glycol reacts with the alkoxides involving intra and intermolecular bonds, leading to the formation of a tridimentional skeleton, favouring the proximity of the metal atoms. The synthesis procedure was the following. The aluminium isopropoxide was solved in propanol and refluxed for 3 h under continuous stirring. After that, the titanium isopropoxide and the ethylene glycol were added and the solution was heated at 70 C. The solution gelled after 1 h. Stirring was stopped and the gel was aged for 5 days, suffering a substantial shrinking. The gel was dried at 100 C for 22 h and calcined, following the program above explained. The molar ratios used in this case were propanol/alkoxide = 15 and ethylene glycol/alkoxide = 3.

2.4. px06Ac

The hydrolysis was controlled by the water generated *in situ*, through the esterification reaction between

propanol and acetic acid, as follows:

$$CH_3\text{-}CH_2OH + CH_3\text{-}COOH \rightarrow CH_3\text{-}COOCH_2\text{-}CH_3 + H_2O$$

This synthesis method has been previously used by other authors [14] in order to moderate the reactivity of the alkoxide for the preparation of ZrO_2. The synthesis procedure was as follows. The aluminium isopropoxide was solved in an appropriate amount of propanol under reflux for 3 h. The amount of propanol used was the difference between the alcohol necessary to keep the alcohol/alkoxide = 15 molar ratio and that necessary to generate by reaction with the acetic acid a number of moles of water involving the water/alkoxide = 5 molar ratio. After that, the solution was cooled at room temperature and the titanium isopropoxide was added. Then, the acetic acid and the rest of propanol were added dropwise, under continuous stirring. The solution gelled after 24 h, meanwhile the precursor px06 did it in a few minutes, as explained previously [12]. This is in line with the results reported for gellification studies of titanium alkoxides solutions by other authors [15], who found that the gelling time increased considerably in the presence of acetic acid. This decrease of the alkoxide reactivity has been attributed to an increment of the co-ordination number of titanium [16]. The reactivity of the Ti(OPr^i) towards the acetic acid can be explained in terms of a nucleophilic substitution of (OPr^i) groups by (OAc) groups. These last are stronger ligands, being able to behave as bidentate, with less steric hindrance than the (OPr^i) groups, leading to an increment of the co-ordination number of titanium from 4 to 6. The OAc groups remain bonded to titanium much longer, and they are hydrolysed more slowly than the OPr^i groups [1, 17].

2.5. px06sep

The hydrolysis of each alkoxide (titanium isopropoxide and aluminium isopropoxide) was carried out separately, according to the same procedure used for the px06 precursor formed by simultaneous hydrolysis, and keeping constant the same molar ratios. Both gels were aged for 5 days, dried in an oven at 80 C for 14 h, and physically grinded and mixed to get the px06sep sample, which was then calcined.

3. Characterisation techniques

The techniques used for the characterization of the samples have been already described [12]. The samples calcined are designed with the same names than the precursors (dried gels) but without the first letter *p*. Thus, for example, the name px06sep is used for a gel dried at 80 C and the name x06sep is employed for the same sample calcined at 500 C.

4. Results and discussion

4.1. Surface and pore size distribution

The textural characteristics of dried and calcined samples are listed in Table I. The BET surface area (S_{BET}), the micropore surface (S_{MIC}) calculated from *t*-plot method [18] and the cumulative meso [19] and micropore [20] volumes are given. The values of S_{BET} of these precursors are substantially lower than that of the px06 precursor prepared by the hydrolytic route. It must be remembered that in the preparation of some of these samples, a precipitate was obtained instead of a gel. It is possible that the reaction between the different alkoxides and the halides has not been completely carried out, and the obtained solid could correspond partly to some of the raw solids that have not completely reacted. Besides, as indicated in the synthesis section, the phaha precursor was not dried, and it is possible it contains ether or $TiCl_4$ occluded into the pores, making them inaccessible to the nitrogen molecules. It can be observed in Table I that when the gels prepared by non-hydrolytic routes are calcined at 500 C, a substantial increment of the S_{BET} values is produced (fundamentally due to a development of the mesoporosity in these samples), with the exception of the haTiIsAl sample, whose surface area is practically the same than that of the dried precursor. The contribution to the S_{BET} values of calcined samples comes from the mesopores, since the values of S_{MIC} obtained by the calculation program are negative, which indicates the absence of micropores. The calcination process leads probably to the removal of a great part of the organic groups occluded into the pores of the gel, resulting in the accessibility of these to the nitrogen molecules. The increase of the mesoporosity produced during the calcination process is also corroborated by comparing the V_{BJH} values of both dried and calcined samples. The samples calcined showing the highest values of S_{BET} (even higher than that of the x06 sample prepared by the hydrolytic route) are the haha

TABLE I Textural characteristics of dried and calcined samples

	Dried samples (80 C)				Calcined samples (500 C)			
Sample	S_{BET} (m^2/g)	S_{MIC} (m^2/g)	V_{BJH} (cm^3/g)	V_{HK} (cm^3/g)	S_{BET} (m^2/g)	S_{MIC} (m^2/g)	V_{BJH} (cm^3/g)	V_{HK} (cm^3/g)
phaha	1.3	—	—	—	262.2	—	0.322	0.098
phaTiSecAl	1.0	—	—	—	200.1	—	0.345	0.075
phaTiIsAl	23.9	—	0.055	0.009	21.2	—	0.059	0.008
pIsTihaAl	2.0	—	0.002	0.001	52.8	—	0.073	0.020
px06	85.3	72	0.014	0.035	178	—	0.248	0.066
px06EG	1.4	—	—	—	34	23.6	0.008	0.013
px06Ac	308	125	0.316	0.124	192	—	0.662	0.073
px06sep	601	233	0.246	0.236	145	—	0.268	0.055

V_{BJH}: mesopore cumulative volume (20–500 Å) from BJH adsorption branch; V_{HK}: micropore volume (<20 Å) from Horvath-Kawazoe.

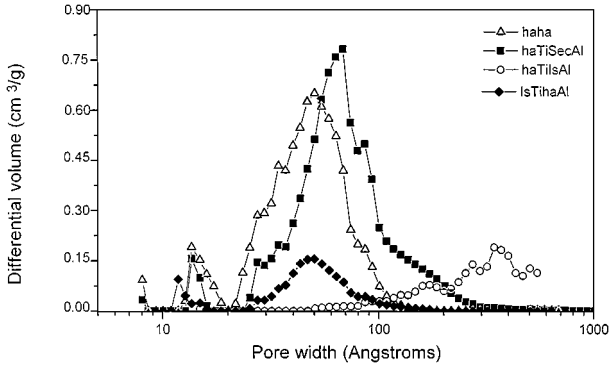

Figure 1 DFT distributions of the $x = 0.6$ samples synthesised by non-hydrolytic routes and calcined at 500 C.

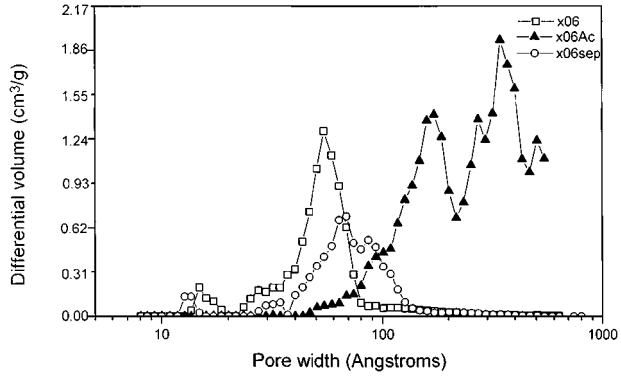

Figure 2 DFT distributions of the $x = 0.6$ samples synthesised with different variables and calcined at 500 C.

and haTiSecAl. It must be remembered that an homogeneous gel is obtained in the preparation of these two samples, in contrast to the precipitate obtained in the preparation of the other two samples.

The Density functional theory (DFT) distributions [21] of those two samples (see Fig. 1) are quite similar between them, showing fundamentally small mesopores (pore size comprised between 20 and 100 Å), with the maxima around 50–65 Å. On the contrary, the haTiIsAl sample contains bigger mesopores (although the pore volume is substantially lower), with a wide pore size distribution between 100 and 600 Å.

With regard to the samples obtained with other synthesis variables, it can be observed in Table I that the S_{BET} values for the precursor synthesised by generation *in situ* of the water (px06Ac) as well as for the formed by physical mixture of the two gels obtained separately (px06sep) are much higher (3.5–7 times) than the S_{BET} value of the px06 sample. In those precursors, the total porosity has been developed, as corroborated if their mesopore (V_{BJH}) and micropore (V_{HK}) volumes values are added and the resulting values are compared with the one obtained for the px06 sample. These samples, px06Ac and px06sep, are fundamentally mesoporous, as deduced by comparation of S_{BET} and S_{MIC} values. The second ones are much lower than the first ones, and the difference between them is the area due to the mesopores. However, the very low S_{BET} value of the precursor of the sample obtained using ethylene glycol (px06EG), may be due to the fact that the drying process of this sample was different. Besides, no water was used to generate the hydrolysis; hence, it is possible that the subsequent polycondensation process occurred in a low degree.

The DFT distributions of these $x = 0.6$ samples calcined at 500 C are plotted in Fig. 2. When the samples are calcined, the pore structure changes, leading to larger diameter pores and decreasing the microporosity. This can be corroborated by comparing the values of V_{BJH} and V_{HK} for both groups of dried and calcined samples. For the x06Ac and x06sep samples, the pore structure collapses and the surface area decreases in a factor of 1.5–4. On the other hand, meanwhile the x06 sample shows a unimodal distribution, the x06sep sample presents a bimodal distribution, with contribution of pores of two sizes, 65 and 90 Å. These last pores could be associated with the contribution of the alumina oxide, which showed the biggest size pore of the $x\mathrm{TiO_2}\cdot(1-x)\mathrm{Al_2O_3}$ series [12]. That is, as the x06sep is formed by the physical mixture of the gels obtained by separated hydrolysis of the two alkoxides, the interaction between the titanium and aluminium atoms to form a mixed has been more hindered, in such way that the contribution to the porosity seems to be the addition of the contributions of both the alumina and the titania. On the other hand, when the hydrolysis is controlled by generation *in situ* of the water, bigger mesopores are formed than in presence of water. Thus, meanwhile the maximum of the distribution of the x06 sample is around 60 Å, the x06Ac sample shows a wide DFT distribution with mesopores of 170, 350 and 500 Å. The DFT distribution of the x06EG sample calcined at 500 C (not shown in the figure because of its different ordinate scale) is practically the same than that of the dried gel (with the maximum of the distribution centred at 25 Å), although its S_{BET} value (whose contribution is principally due to the micropores, being the S_{BET} and S_{MIC} values very similar) is around 10 times higher.

4.2. Thermal behaviour

The thermograms of the four samples prepared by non-hydrolytic routes and dried at 80 C are depicted in Fig. 3a, together with that of the px06 precursor prepared by the hydrolytic route. All the samples undergo a mass loss higher than that of the px06 sample, indicating a lower degree of condensation in those samples. For the five gels, the thermal degradation occurs in the same temperature range. The mass losses vary from 37.0 to 53.7 wt % as a function of the degree of condensation of the gels and the nature of the OR group. When the $TiCl_4$ is used, no significant change results from the nature of the aluminium alkoxide used (secbutoxide or isopropoxide), in such way that the TG curves of both samples (phaTiSecAl and phaTiIsAl) lead to very similar residue values (54–55 wt %). The profiles of both curves are different, however, and from 200 C the curve of the precursor containing secbutoxide is shifted around 100 C towards higher temperatures than that of the precursor containing isopropoxide. Nevertheless, the fact that the final weight losses of both samples are very similar, indicates that there is no significant difference in the degree of condensation of the gel, that

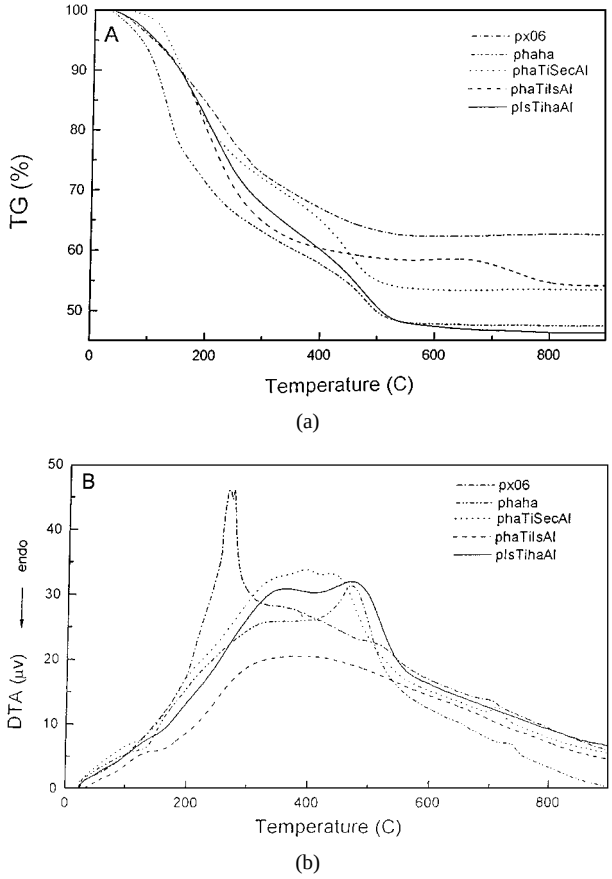

Figure 3 Thermal analyses for the $x = 0.6$ precursors synthesised by non-hydrolytic routes (for comparison, px06 is also included). A: TG curves; B: DTA curves.

is, this is not influenced by the nature of the aluminium alkoxide.

The gels show a very similar weight loss (∼14 wt %) up to 200 C, with the exception of phaha, which undergoes a higher weight loss (27 wt %), probably due to the removal of the diisopropyl ether physically adsorbed (B.P. = 71 C). The TG curve of this last sample shows a first loss zone of ∼22 wt % up to 125 C, which is assigned to the elimination of the physisorbed water and ether. There is a second step (slower than the first one) from 125 C onwards, which may be assigned to the loss of the remaining $TiCl_4$ (B.P. = 136 C) and to the thermal decomposition and oxidation of the remaining alkoxide groups. On the other hand, the use of CCl_4 as solvent of either the aluminium isopropoxide or the aluminum trichloride was necessary for the synthesis of the phaTiIsAl and pIsTihaAl precursors. Both samples show TG curves with a very similar profile, almost overlapped up to 400 C, with an associated weight loss of 40 wt %. The profiles are quite different, however, from this temperature onwards and the final weight loss of phaTiIsAl sample is almost 8 wt % higher than the one of the pIsTihaAl sample. In this case, the fact that the oxygen donor is the titanium alkoxide or the aluminium alkoxide seems to have an effect on the condensation degree. Other authors [11b] also observed different residues in the TG curves of Ti-Zr gels, as a function of either the use of titanium alkoxide and zirconium halide or the use of titanium halide and zirconium alkoxide.

The weight losses occurring between 200 and 500 C, assigned to the thermal decomposition of the alkoxide groups and to the oxidation of the remaining groups, are associated with some broad exothermic peaks in the DTA curves (see Fig. 3b), which have very similar profiles to those of Ti-Zr gels prepared in a similar way by other authors [11a]. At the same time, they are very different and worse defined than that corresponding to the sample prepared by the hydrolytic way (px06). In general, in Fig. 3b, two exothermic peaks can be observed in the 300–500 C range, centred at around 340 C and 460 C, respectively (see Table II). Additionally, a third exothermic peak of less intensity appears centred at 732 and 713 C for the phaha and phaTiSecAl samples, respectively, and this has been attributed to the crystallization process of the oxides phases, as will be shown in the DRX studies. This peak is not observed in the DTA curves of the phaTiIsAl and pIsTihaAl precursors, although these two samples are, however, amorphous at 500 C and incipient crystalline at 750 C. Probably, the value of the heat evolved in their crystallization process is not large enough to be detected by the DTA technique. This crystallization process was observed to occur at a lower temperature (696 C) for the sample prepared by the hydrolytic way (px06) [12]. The profile of the DTA curve of this last sample is very different and shows a doublet of very sharp and intense exothermic peaks, centred at 263 an 271 C, associated with the decomposition of the titanium isopropoxide and the aluminium isopropoxide [12], respectively (see Table II).

The TG curves for the $x = 0.6$ samples prepared with other synthesis variables are depicted in Fig. 4a. Three

TABLE II Temperature (C) of the maxima of DTA curves for the $x = 0.6$ precursors synthesised by different routes and for IsopTi and IsopAl

Sample	Temperature (C)						[a]
IsopTi	—	234 (endo) 243	—	—	374	—	765
IsopAl	140 (endo)	—	281	—	—	—	836; 854
phaha	140 (endo)	—	—	324	—	467	732
phaTiSecAl	133 (endo)	—	—	340	394	440	713
phaTiIsAl	131	—	—	—	376	—	—
pIsTihaAl	—	—	—	356	—	475	—
px06	—	263	271	—	—	—	696
px06EG	185	—	—	310	—	—	758
px06Ac	—	—	288 (endo)	—	379	—	—
px06sep	175	220; 243	277	316	—	—	498

All the peaks are exothermic, if the opposite is not indicated.
[a]Temperature associated with the crystallization process or phase transformation.

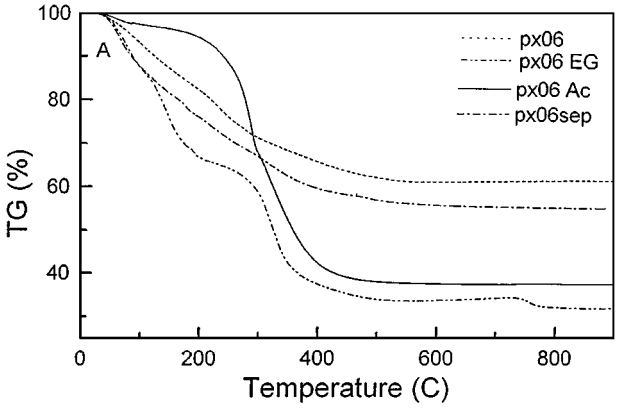

(a)

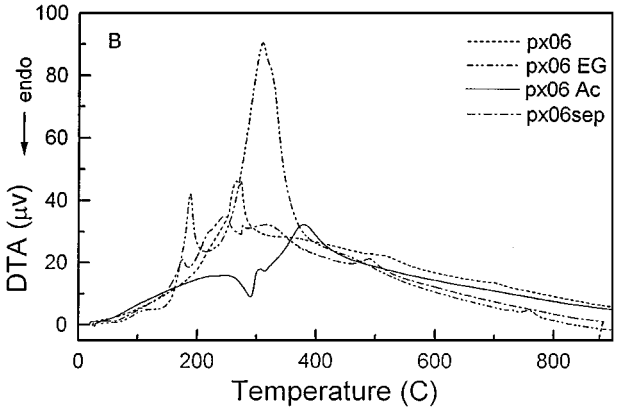

(b)

Figure 4 Thermal analyses for the $x = 0.6$ precursors synthesised with different variables. A: TG curves; B: DTA curves.

well-defined weight loss steps can be observed in the TG curve of the sample prepared with ethylene glycol (px06EG). The first step (12 wt %) until around 100 C can correspond to the loss of both physisorbed water and alcohol. The second one (23 wt %) occurs in the 100–250 C range and may be associated with the removal of the physisorbed ethylene glycol (B.P. = 196 C). Additionally, there is a third weight loss step from 600 C onwards, which could be assigned to the decomposition of the complex formed and to the pyrolysis of the remaining organic groups. The TG curve of the sample prepared by generation *in situ* of the water (px06Ac) also displays a profile with three-well defined weight loss steps: a first one (5 wt %) very slow until 200 C, and two ones faster around 24 wt % each one (in the 200–300 C and 300–400 C ranges). For this sample, the decomposition is initiated a little bit later (which indicates the higher stability of the gel formed by generation *in situ* of the water) and it occurs in a narrower temperature range, which is more defined than in the case of the samples prepared in presence of water (px06 and px06sep). The TG curve of the precursor formed by physical mixture of the gels obtained by separated hydrolysis of the two alkoxides (px06sep) shows a profile quite similar to that of the precursor originated by simultaneous hydrolysis (px06). However, the first curve is shifted 90–100 C towards lower temperatures and leads to a final weight loss higher than the second one. The fact that the decomposition of the px06sep precursor is initiated before than that of the px06 precursor is an indication of the higher thermal stability of the gel prepared by simultaneous hydrolysis. Besides, this last gel seems to have a higher degree of condensation and, therefore, a lower number of residual alkoxide groups than the gel obtained by separated hydrolysis, as corroborated by the lower weight loss experimented by the first sample (px06).

The corresponding DTA curves of the $x = 0.6$ precursors prepared by hydrolytic ways are depicted in Fig. 4b and the temperatures of the maxima are listed in Table II. The DTA curve of the sample prepared with ethylene glycol as complexing agent (px06EG) displays two very intense exothermic peaks, centred at 185 and 310 C, respectively. These are well corresponded with two defined weight losses observed in the TG curve. In the case of the sample prepared by physical mixture of the two gels of titanium and aluminium (sample px06sep), some exothermic peaks badly defined are observed in the 200–300 C zone, and they correspond to the decomposition of the two respective raw alkoxides (see Table II). Both peaks are more separated in the DTA curve of this sample than in the DTA curve of the sample obtained by simultaneous hydrolysis (px06). This is a consequence of the existence of two gels in the first case, each one proceeding from the hydrolysis of its respective alkoxide. Furthermore, in the DTA curve of the px06sep precursor, there is an exothermic peak centred at 488 C, which corresponds to a constant weight region in the TG curve. For this reason, this peak has been assigned to the formation of a crystalline phase from an amorphous precursor, as will be corroborated by the DRX studies. This fact means that the precursor obtained by physical mixture of the two gels crystallises at a temperature that is 200 C lower than that of the precursor formed by the simultaneous hydrolysis.

4.3. Crystalline phases

The diffraction patterns of the four samples prepared by non-hydrolytic routes and calcined at 500 C (not shown) indicate that all are amorphous, likewise the sample prepared by the hydrolytic way (px06) is. As an exothermic peak is observed around 700 C in the DTA curves of the phaha and phaTiSecAl samples (see Table II), it was decided to calcine the four non-hydrolytic samples at 750 C, in order to inquire more about the nature of the phases formed above this temperature. The corresponding diffractograms of the samples calcined at 750 C are depicted in Fig. 5. It can be observed that in all cases where a halide and an alkoxide have been used for the synthesis, a mixture of different phases is obtained. Thus, in the case of haTiIsAl and IsTihaAl samples, two different aluminium oxides, with hexagonal and cubic structures are formed. For the haTiSecAl sample, the majority phase formed is the anatase, although the mixed oxide Al_2TiO_5 is also obtained. However, as noticed in Fig. 5, when the synthesis has been carried out from the mixture of the two metal halides and diisopropyl ether (haha), a unique phase of the Al_2TiO_5 mixed oxide is obtained, instead of a mixture of phases. Therefore, the halide-halide-ether route seems to lead

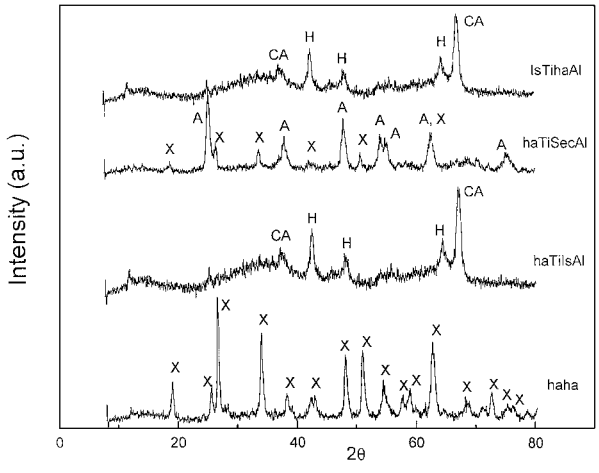

Figure 5 X-ray diffraction patterns of the $x = 0.6$ samples synthesised by non-hydrolytic routes and calcined at 750 C. A: anatase; X: Al_2TiO_5; H: hexagonal Al_2O_3; CA: cubic Al_2O_3.

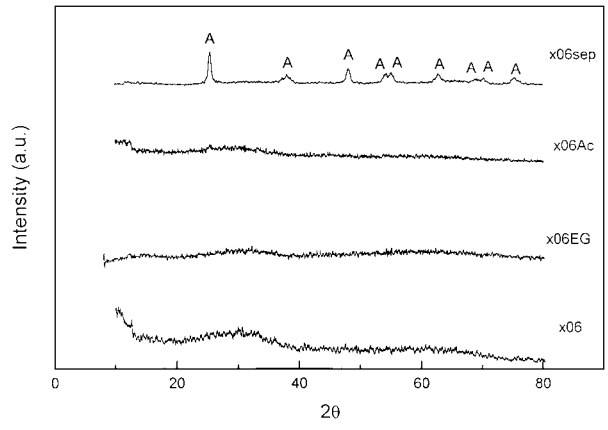

Figure 6 X-ray diffraction patterns of the $x = 0.6$ samples synthesised with different variables and calcined at 500 C. A: anatase.

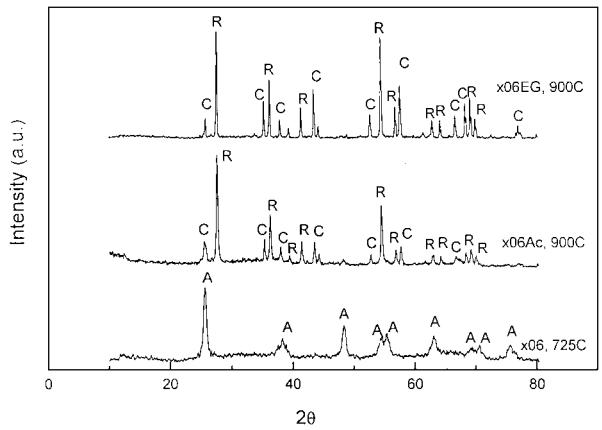

Figure 7 X-ray diffraction patterns of the $x = 0.6$ samples synthesised with different variables and calcined at different temperatures. A: anatase; R: rutile; C: corundum (α-Al_2O_3).

to a gel with higher degree of homogeneity than the formed with the halide-alkoxide route. A possible explanation can be based in the fact that the chloride atoms can act as mineraliser, namely facilitate diffusion in the solid state, thus promoting the formation of mixed oxides. From the equations of synthesis of the precursors (see Synthesis procedure section), it can be noticed that the amount of chloride per metal atom for the halide-halide-ether route is double than that used in the halide halide-alkoxide reactions. Therefore, at higher chloride amount, higher homogeneity of the mixed oxide. The promoting effect of the chloride atoms seems to agree with the fact observed by other authors that the crystallization process of the $TiZrO_4$ mixed oxide occurred at 705 C for gels prepared by hydrolysis of metal alkoxides [22], meanwhile it was produced at a lower temperature (640 C) for gels obtained from metal chlorides [23]. Nevertheless, although the amounts employed in the synthesis of haha sample were the appropriate to obtain the mixed oxide equivalent to a molar ratio of $x = 0.6$, the oxide obtained seems to be deficient in titania, because its stoichiometry corresponds to a molar ratio of $x = 0.5$.

The diffractograms of the $x = 0.6$ samples prepared with different synthesis variables and calcined at 500 C are depicted in Fig. 6. It can be observed that all the samples are amorphous, with the exception of the x06sep sample, which shows diffraction peaks assigned to the anatase phase. The corresponding DTA curve of this precursor (see Fig. 4b) shows an exothermic peak centred at 488 C, associated with a constant weight region, which has been assigned to the crystallization process of the amorphous TiO_2 into anatase. According to this result, it can be concluded that the precursor formed by physical mixture of the two gels crystallises at a temperature 200 C lower than that of the precursor formed by simultaneous hydrolysis (crystallization temperature of the x06 sample = 696 C) [12]. Other authors [24] also found a decrease of 80 C in the crystallization temperature of a $0.2TiO_2{\cdot}(1-x)Al_2O_3$ sample prepared by separated hydrolysis with respect to that of the same sample obtained by simultaneous hydrolysis. Taking into account the temperatures observed in the DTA curves (see Table II) and in order to inquire more about the phases formed above these temperatures, the px06 sample was calcined at 750 C and the px06EG and px06Ac samples were calcined at 900 C. The diffractograms of these samples calcined at high temperatures are depicted in Fig. 7. It can be noticed that a mixture of two phases, rutile and α-Al_2O_3, is obtained for both x06EG and x06Ac samples. These two also phases were observed in the difractogram of the $0.2TiO_2{\cdot}0.8Al_2O_3$ sample calcined at 900 C, as reported previously [12]. Therefore, the presence of titanium seems to favour the transformation of γ-Al_2O_3 into α-Al_2O_3 at a temperature near 900 C, which is lower than that reported for the pure alumina by other authors [25, 26]. The results found by us are in agreement with others reported previously [27–31], which showed that the presence of oxides such as Fe_2O_3, TiO_2, MgO, NiO, CuO, MnO_2, V_2O_5 and PtO promoted the formation of α-Al_2O_3 at temperatures close to 900 C. In any case, meanwhile a mixture of simple oxides is obtained by us in the samples prepared with different variables by hydrolytic routes, a mixed oxide is formed in two of the samples synthesised by non-hydrolytic routes. Therefore, the non-hydrolytic route seems to favour a closer interaction between the two metallic precursors, probably due to the mineraliser effect of chloride atoms.

TABLE III ZPC values of the $x = 0.6$ samples calcined at 500 C

Sample	haha	haTiSecAl	haTiIsAl	IsTihaAl	x06	x06EG	x06Ac	x06sep
ZPC	4.3	4.9	5.1	5.0	5.2	4.1	6.3	5.2

4.4. Zero point charge (ZPC) values

In the mixed oxide systems it is interesting to determine the surface distribution of the two oxides and its dependence upon the overall composition, and the technique of electrophoretic migration has been proved to be very sensitive to the variations in the surface coverage for a number of supported catalysts systems. The ZPC values of the $x = 0.6$ samples prepared in the present work are listed in Table III. It can be observed that, in general, with the exception of the haha sample, the samples prepared by non-hydrolytic routes have ZPC values very close to that of the sample prepared by the hydrolytic way (x06), which indicates that the composition at the surface of these all samples is very similar. Besides, these ZPC values are well adjusted to the straight-line equation relating the ZPC values of the mixed oxide with the molar fraction and the isoelectric point of the simple oxides [12]. This fact indicates that the surface distribution of the oxides follows the bulk composition of the corresponding mixed oxides. The sample prepared from the two metal halides and diisopropyl ether (haha) has, however, a ZPC value almost 1 unity lower than that of the x06 sample. It must be remembered that this sample haha has also a different composition at the bulk, because the calcination at 750 C leads to the formation of a unique crystalline phase, the Al_2TiO_5 mixed oxide, whose stoichiometry corresponds to the $x = 0.5$ molar ratio, instead of $x = 0.6$.

On the other hand, the ZPC value of the sample prepared by physical mixture of the two gels (x06sep) is exactly equal to the value corresponding to the sample prepared by simultaneous hydrolysis (x06). This fact indicates that the composition at the surface of both samples is the same, in spite of the different pore structure and crystalline composition (the first sample contains anatase meanwhile the second one is amorphous). Conversely, the samples prepared with ethylene glycol (x06EG) and by generation *in situ* of water (x06Ac) have ZPC values which deviate in almost one unity from the ZPC value of the x06 sample. Thus, the ZPC value of the x06EG sample is lower (4.1) than that of the x06 sample, hence, close to that corresponding to a sample with higher titania content. However, the ZPC value of the x06Ac sample is much higher (6.3) and close to that corresponding to a sample with higher alumina content. Therefore, although the stoichiometry composition at the bulk of these three samples is the same, the composition at the surface seems to be very different, being quite influenced by the preparation method.

4.5. Surface acidity

As indicated previously [12] a potentiometric method of titration with *n*-butylamine was used to characterize the surface acidity [32]. The titration curves of the

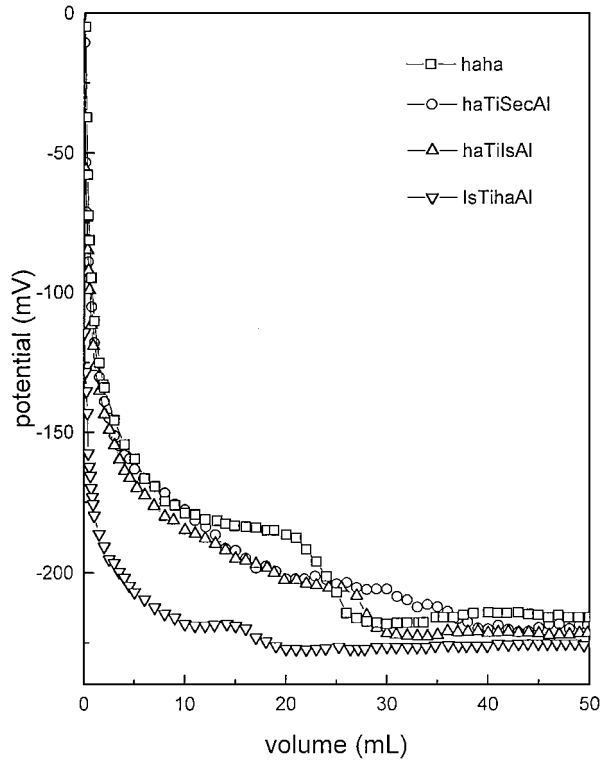

Figure 8 Titration curves with *n*-butylamine for the $x = 0.6$ samples synthesised by non-hydrolytic routes and calcined at 500 C.

$x = 0.6$ samples prepared by non-hydrolytic routes are depicted in Fig. 8 and the results of the titrations are listed in Table IV. Together with the initial electrode potential (E_0) and the potential decrease (ΔV) values, the acid sites surface density is given (the subscripts 1 and 2 referee to first and second step, respectively). According to the method used, the E_0 value indicates the maximum acid strength of the first titrated surface acid sites. It can be observed that the sample containing the strongest acid sites of the four non-hydrolytic samples is the one prepared from the two halides and diisopropyl ether (haha). Its E_0 value (65 mV, not displayed in Fig. 8) is, at the same time, the closest to the E_0 value of the x06 sample prepared by the hydrolytic way. It must be remembered that the gel of highest homogeneity was obtained during the preparation of the haha sample and a unique phase of mixed oxide was obtained. On the other hand, the higher the potential decrease produced during the titration, the higher is the difference of acidity between the initial and the final acid sites of each step of the titration curve. Two well-defined steps can be differentiated in the titration curve of the haha sample. There is a first type of strongest acid sites, titrated until around 15 mL, with a great acidity difference between the initial and the final acid sites (potential decrease of 250 mV). A second type of sites with less acid strength is titrated between 20 and 30 mL. The haTiIsAl and IsTihaAl samples seem also to contain two types of acid sites, because two steps are

TABLE IV Results of the titration with *n*-butylamine of the $x = 0.6$ samples calcined at 500 C and acid sites surface density

Sample	E_0 (mV)	S_{BET} (m^2/g)	ΔV_1 (mV)	meq_1/m^2	ΔV_2 (mV)	meq_2/m^2
haha	65	262	250	0.092	32	0.051
haTiSecAl	−37	200	210	0.259	—	—
haTiIsAl	−10	21	171	1.631	14	0.251
IsTihaAl	−41	53	167	0.302	12	0.126
x06	136	178	297	0.075	—	—
x06EG	−95	34	121	0.590	—	—
x06Ac	−104	192	105	0.055	33	0.069
x06sep	−94	145	110	0.074	27	0.092

The subscripts 1 and 2 referee to first and second steps, respectively.

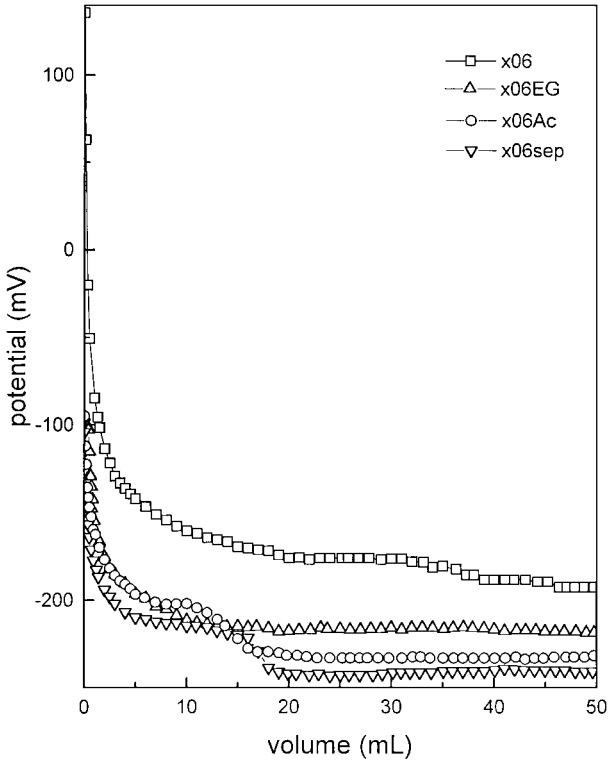

Figure 9 Titration curves with *n*-butylamine for the $x = 0.6$ samples synthesised with different variables and calcined 500 C.

observed in their respective titration curves, although less differentiated that in the case of haha sample. As reported in Table IV, the surface density of the strongest acid sites (titrated during the first step) is, in both cases, higher than that of the weakest acid sites (titrated during the second step). The haTiIsAl sample is the one having the lowest surface area of all the samples, but it is the one containing the highest total surface density of acid sites (1.882 meq/m^2). The haTiSecAl sample shows a very wide and little defined distribution of acid sites, and the potential value shows a continuous decrease, in such way that the titration curve does not reach the plateau until the addition of 39 mL of basic solution.

With regard to the $x = 0.6$ samples prepared with different variables, their titration curves are depicted in Fig. 9 and the results of these titrations are listed in Table IV. According to the initial potential values (E_0), it can be observed that the strongest acid sites of the samples are of a very similar acid strength; at the same time, they are quite weaker than those of the x06 sample, whose E_0 value is much higher. The titration curves of the x06Ac and x06sep samples seem to reach a first plateau around 8 mL, and after that, a second drop between 10 and 20 mL is observed. These two samples seem to contain, therefore, two types of acid centres of different strength (they also showed pores of two different sizes in the DFT distribution). The two steps observed in the titration curve of the x06sep sample (prepared by physical mixture of the two gels) could be probably due to the contribution of the corresponding acid sites of each simple oxide (TiO_2 and Al_2O_3). Besides, it must be remembered that this sample showed a bimodal distribution of pores size, with contribution of both simple oxides. On the contrary, in the case of the sample prepared by simultaneous hydrolysis of the two alkoxides (x06), a wide distribution of mixed acid sites seems to exist, because its corresponding titration curve shows a continuous drop without differentiation between some well-defined steps. The existence of the mixed acid sites is probably due to a higher homogeneity of the gel, which leads to the formation of bridged hetero metal-oxygen bonds (Ti-O-Al). The sample prepared with ethylene glycol (x06EG) seems to contain a unique type of acid sites of well defined strength, because its titration curve reaches the plateau around 15 mL (17.3 meq/g).

As indicated before, the higher the potential decrease, the higher is the difference of acidity between the initial and the final acid sites of each step of the titration curve. On the contrary, very small potential decreases indicate a very similar acid strength for both types of acid sites. In this way, the three samples (x06Ac, x06EG and x06sep) not only have the strongest acid sites of a very similar strength (their E_0 values are very similar), but they also contain a similar distribution of the strongest acid sites, because the potential decrease ΔV_1 produced in the first step is very similar in the three cases. The same conclusion can be applied to the second step of the titration curves of the x06Ac and x06sep samples (ΔV_2 around 30 mV). On the other hand, although the *n*-butylamine consumption for each step is very similar for all the samples, as the surface areas are quite different, different surface densities of the acid sites are also obtained. Thus, the sample containing the highest density is the one prepared with the complexing agent (x06EG).

5. Summary and conclusions

A series of $0.6TiO_2 \cdot 0.4Al_2O_3$ catalytic supports has been prepared by different sol-gel methods. The non-hydrolytic method has allowed us to obtain some

samples whose surface areas are higher than that of the sample prepared by the hydrolytic way. Besides, the synthesis method has an effect on the pore size distribution of the support obtained. Thus, the use of acetic acid for the generation in situ of the hydrolysis water, or the separated hydrolysis of the alkoxides, leads to the formation of higher mesopores than those of the x06 sample, specially in the case of the x06Ac sample, whose maximum of the DFT distribution is around 300 Å. Meanwhile the samples prepared by non-hydrolytic routes and x06 samples show a unimodal pore size distribution, the x06Ac and x06sep samples present a wider pore size distribution, with some maxima. Some differences are observed in the thermal behaviour of the samples, depending on the synthesis method used, although all the samples seem to have a lower condensation degree than that of the x06 sample. The gel originated by simultaneous hydrolysis has a higher thermal stability than that formed by physical mixture of the alkoxides hydrolysed separately. The nature of the aluminium alkoxide used seems not to affect the condensation degree of the samples prepared by non-hydrolytic routes. However, this is influenced by the fact that the oxygen donor is either the titanium alkoxide or the aluminium alkoxide. A mixture of different phases is obtained after the calcination process in most of these samples. However, the difractogram of the sample prepared by the halide-halide-ether route and calcined at 750 C reveals the presence of a unique phase, the Al_2TiO_5 mixed oxide. Probably, the promoting effect of the chloride atoms causes a higher diffusion in the solid state of the two metallic precursors, leading to a higher homogeneity of the gel. The mixed oxide Al_2TiO_5 is also formed in the calcination at high temperature of the haTiSecAl sample prepared by other non-hydrolytic route, at difference of the samples synthesised by hydrolytic routes, which contain a mixture of simple oxides. The samples synthesised in this work contain acid sites which are weaker than those of the x06 sample prepared by the hydrolytic way. Most of the samples seem to contain two quite defined types of acid sites, in contrast to the x06 sample, which exhibits a very wide distribution of acid sites.

References

1. C. SÁNCHEZ and J. LIVAGE, *New. J. Chem.* **14** (1990) 513.
2. C. J. BRINKER, D. E. CLARK and D. R. ULRICH, in "Better Ceramics Through Chemistry," Vol. 73 (Materials Research Society, Pittsburgh, 1986) p. 820.
3. W. ZHANG and F. P. GLASSER, *J. Mater. Sci.* **28** (1993) 1129.
4. T. KLIMOVA, M. L. ROJAS, P. CASTILLO, R. CUEVAS and J. RAMIREZ, *Microporous Mesoporous Mater.* **20** (1998) 293.
5. T. LÓPEZ, A. ROMERO and R. GOMEZ, *J. Non-Cryst. Solids* **127** (1991) 105.
6. K. BALAKRISHNAN and R. D. GONZÁLEZ, *J. Catal.* **144** (1993) 395.
7. A. Z. KHAN and E. RUCKENSTEIN, *Appl. Catal.* **90** (1992) 199.
8. M. L. ROJAS-CERVANTES, A. J. LÓPEZ-PEINADO, J. DE D. LÓPEZ-GONZÁLEZ and F. CARRASCO-MARÍN, *J. Mater. Sci.* **31** (1996) 437.
9. L. G. HUBERT-PFALZGRAF, *New. J. Chem.* **11** (1987) 663.
10. M. L. ROJAS-CERVANTES, R. M. MARTÍN-ARANDA, A. J. LÓPEZ-PEINADO and J. DE D. LÓPEZ-GONZÁLEZ, *J. Mater. Sci.* **29** (1994) 3743.
11. a) M. ANDRIANAINARIVELO, R. J. P. CORRIU, D. LECLERCQ, P. HUBERT MUTIN and A. VIOUX, *J. Mater. Chem.* **6**(10) (1996) 1665; b) *ibid.* **7**(2) (1997) 279.
12. R. LINACERO, M. L. ROJAS-CERVANTES and J. DE D. LÓPEZ-GONZÁLEZ, *J. Mater. Sci.* **35** (2000) 3279.
13. K. MOEDRITZER, in "Organometallic Reactions," Vol. 2, edited by E. I. Becker and M. Tsutsui (Wiley Interscience, 1971) p. 1.
14. C. GUIZARD, N. CYGANKIEWICZ, A. LANBOT and L. COT, *J. Non-Cryst. Solids.* **82** (1986) 86.
15. S. DOEUFF, H. M. SÁNCHEZ and J. LIVAGE, *ibid.* **89** (1987) 206.
16. J. LIVAGE, C. SÁNCHEZ, M. HENRY and S. DOEUFF, *Solid State Ionics* **32/33** (1989) 633.
17. C. SÁNCHEZ, J. LIVAGE, M. HENRY and F. BABONNEAU, *J. Non-Cryst. Solids* **100** (1988) 65.
18. B. C. LIPPENS and J. H. DE BOER, *J. Catal.* **4** (1965) 319.
19. E. P. BARRET, L. S. JOYNER and P. P. HALLENDA, *J. Am. Chem. Soc.* **73** (1952) 373.
20. G. HORVARTH and K. KAWAZOE, *J. Chem. Eng. Japan* **16**(6) (1983) 470.
21. J. P. OLIVIER, *J. Porous Mater* **2** (1995) 9.
22. L. BONHOMME-COURY, N. LEQUEUX, S. MUSSOTTE and P. BLOCH, *J. Sol-Gel Sci. Technol.* **2** (1994) 371.
23. J. A. NAVÍO, F. J. MARCHENA, M. MACÍAS, P. J. SÁNCHEZ-SOTO and P. PICHAT, *J. Mater. Sci.* **27** (1992) 371.
24. M. TOBA, F. MIZUKAMI, S. I. NIWA, Y. KIYOZUMI, K. MAEDA, A. ANNILA and V. KOMPPA, *J. Mater. Chem.* **414** (1994) 585.
25. B. C. LIPPENS and J. H. DE BOER, *Acta Crystallogr.* **17** (1964) 1312.
26. H. S. SANTOS and P. S. SANTOS, *Mater. Lett.* **13** (1992) 175.
27. Y. WAKAO and T. HIBINO, *Nagoya Kogyo Gijutsu Schimanko Hokoku* **11** (1962) 588.
28. G. C. BYE and G. T. SIMPKIN, *J. Am. Ceram. Soc.* **57** (1974) 367.
29. N. S. KURKOVA, Y. R. KATSOBASHVILI and N. A. AKCHURINA, *Zh. Prikl.* **46** (1973) 1002.
30. N. S. KOZLOV, M. Y. LAZAREV, L. MOSTOVAYA and I. P. STREMOK, *Kinet. Catal.* **14** (1973) 1130.
31. a) P. BURTIN, J. P. BRUNELLE, M. PIJOLAT and M. SOUSTELLE, *Appl. Catal.* **24** (1987) 239; b) *ibid.* **34** (1987) 225.
32. R. CID and G. PECCHI, *Appl. Catal.* **14** (1985) 15.

Received 27 May
and accepted 18 November 1999